Electromagnetics, 1989
pp 169-186

Sensor and Simulation Note
Note 309
September 1987

Perturbation of the SEM-Pole Parameters of an Object by a Mirror Object

Carl E. Baum
Air Force Weapons Laboratory

Thomas H. Shumpert
Lloyd S. Riggs
Auburn University

Abstract

Given the natural frequencies of an object (electromagnetic atterer) in free space, one can consider how they are changed the presence of another object in its proximity. This note considers the case that the second object is symmetrical with respect to the first with a plane of symmetry between them. A perturbation of the natural frequencies is found which is applicable to an intermediate range of spacing between them.

Acknowledgements

The authors would like to thank Mr. John L. Lindsey of the Electrical Engineering Department of Auburn University for his help in carrying out the computations presented in the numerical examples contained in this report.

Contents

I. Introduction

In the SEM literature there is some peculiar behavior of the natural frequencies of an object when it is placed in the presence of a perfectly conducting plane [2,3,6,9,11]. Specifically we are referring to the spiral behavior of the natural frequencies as the distance of the object from the ground plane is varied. Thinking that the interaction of the object with its image ought to be weak, at least under some conditions, the idea occurred of some kind of perturbation analysis, such as is used in quantum mechanics.

Generalizing the problem let us consider an object with its mirror object, i.e. let there be two objects symmetrical with respect to a plane. A symmetry plane implies that the electromagnetic scattering divides into two non-interacting parts, denoted symmetric and antisymmetric. The antisymmetric part also applies to the case that this symmetry plane is replaced by a perfectly conducting plane with no mirror object present.

This paper discusses the SEM-pole parameters under the conditions of such symmetry. Separating terms according to those for a single object and for the interaction of two symmetrical objects, perturbation theory is next applied. An approximate formula for the perturbation of natural frequencies is thereby derived.

II. SEM Poles

Write the SEM form of the surface current density on a finite-dimension, perfectly conducting object in free space as

$$\vec{J}_s(\vec{r}_s,t) = E_0 \sum_\alpha \tilde{f}_p(s_\alpha)\eta_\alpha \vec{j}_{s_\alpha}(\vec{r}_s)e^{s_\alpha t}u(t-t_0)$$

$$+ \text{ other SEM terms + noise}$$

$$\tilde{\vec{J}}_s(\vec{r}_s,s) = E_0 \sum_\alpha \tilde{f}_p(s_\alpha)\eta_\alpha \vec{j}_{s_\alpha}[s-s_\alpha]^{-1}e^{-(s-s_\alpha)t_0}$$

$$+ \text{ other SEM terms + noise} \qquad (2.1)$$

t_0 ≡ turn-on time

$\vec{j}_{s_\alpha}(\vec{r}_s)$ ≡ natural mode (appropriately normalized)

s_α ≡ natural frequency

η_α ≡ coupling coefficient (taken as class 1 for present purposes)

$\tilde{f}_p(s)$ ≡ Laplace transform of incident waveform $f_p(t)$

E_0 ≡ scaling constant for incident wave (in V/m)

$\vec{r}_s$ ≡ coordinate on the surface S of the object

The coupling coefficient η_α contains information concerning the incident fields (plane wave or otherwise). However, pole locations and natural modes have nothing to do with the incident fields.

Now the interaction of incident fields with the scatterer can be formulated as an integral equation of the form

$$\langle \tilde{\overleftrightarrow{T}}(\vec{r}_s,\vec{r}'_s;s) \;;\; \tilde{\vec{J}}_s(\vec{r}'_s,s)\rangle = \tilde{\vec{I}}(\vec{r}_s,s) \tag{2.2}$$

$\langle\ ;\ \rangle \equiv$ symmetric product (integration of common spatial coordinates over S)

$\tilde{\overleftrightarrow{T}}(\vec{r}_s,\vec{r}'_s;s) \equiv$ dyadic kernel

$\tilde{\vec{I}}(\vec{r}_s,s) \equiv$ incident-field related quantity

with multiplication in this case in the dot-product sense. There are various forms of integral equations that have been used involving incident electric fields, magnetic fields, combinations of these, etc. In each case there is a different dyadic kernel in the integral equation.

For present purposes we use the impedance or E-field integral equation

$$\langle \tilde{\overleftrightarrow{Z}}(\vec{r}_s,\vec{r}'_s;s) \;;\; \tilde{\vec{J}}_s(\vec{r}'_s,s)\rangle = \tilde{\vec{E}}(\vec{r}_s,s) \tag{2.3}$$

where $\tilde{\vec{E}}_s$ is some "source" electric field, such as an incident field or some specified field such as at an antenna gap. Note that both $\tilde{\vec{J}}_s$ and $\tilde{\vec{E}}_s$ are tangential to S.

This impedance kernel is connected to the dyadic Green's function of free space as

$$\tilde{\overleftrightarrow{Z}}(\vec{r}_s,\vec{r}'_s;s) = s\mu_0 \overleftrightarrow{I}_t(\vec{r}_s)\cdot\tilde{\overleftrightarrow{G}}_0(\vec{r}_s,\vec{r}'_s;s)\cdot\overleftrightarrow{I}_t(\vec{r}'_s)$$

$\vec{I}_S(\vec{r}_s) \equiv$ unit normal to S at $\vec{r}_s$ (2.4)

(outward pointing for oriented (or two-sided) surface)

$\overleftrightarrow{I} \equiv \vec{I}_x\vec{I}_x + \vec{I}_y\vec{I}_y + \vec{I}_z\vec{I}_z \equiv$ identity dyad

$$\overleftrightarrow{I}_t(\vec{r}_s) = \overleftrightarrow{I} - \vec{I}_S(\vec{r}_s)\vec{I}_S(\vec{r}_s) \equiv \text{transverse dyad at } \vec{r}_s \text{ on S}$$

It is convenient to define the impedance kernel in terms of components tangential to S via $\vec{I}_S$ when dealing with fields on S (i.e. $\vec{r} = \vec{r}_s$). For fields away from S this part is conveniently dropped, i.e. just $s\mu_0\tilde{\overleftrightarrow{G}}_0$ is used.

The scalar Green's function is given by

$$\tilde{G}_0(\vec{r}_s,\vec{r}'_s;s) = \gamma \frac{e^{-\zeta}}{4\pi\zeta} \tag{2.5}$$

$$\gamma = \frac{s}{c} \qquad \text{(propagation constant)}$$

$$c = (\mu_0\epsilon_0)^{-\frac{1}{2}} \qquad \text{(speed of light)}$$

$$Z_0 = \left(\frac{\mu_0}{\epsilon_0}\right)^{\frac{1}{2}} \qquad \text{(wave impedance)}$$

$$R = |\vec{r}_s - \vec{r}'_s|$$

$$\zeta = \gamma R$$

from which we obtain the dyadic Green's function

$$\begin{aligned}\tilde{\overleftrightarrow{G}}_0(\vec{r}_s,\vec{r}'_s;s) &= [\overleftrightarrow{I} - \gamma^{-2}\nabla\nabla]\tilde{G}_0(\vec{r}_s,\vec{r}'_s;s) \\ &= \frac{\gamma}{4\pi}\{[-2\zeta^{-3} - 2\zeta^{-2}]e^{-\zeta}\vec{I}_R\vec{I}_R \\ &\quad + [\zeta^{-3} + \zeta^{-2} + \zeta^{-1}]e^{-\zeta}[\overleftrightarrow{I} - \vec{I}_R\vec{I}_R]\} \\ &\quad + \gamma^{-2}\vec{I}_S\vec{I}_S\delta(\vec{r} - \vec{r}'_s)\end{aligned} \tag{2.6}$$

$$\vec{I}_R = \frac{\vec{r}_s - \vec{r}'_s}{|\vec{r}_s - \vec{r}'_s|} \qquad (\text{for } \vec{r}_s \neq \vec{r}'_s)$$

Here we have included the integration near $\vec{r} = \vec{r}_s'$ as given by Yaghjian [8]. This is not the only form it can take, but it is not important for present considerations. The transverse dyad in (2.4) removes this term. The integration in (2.3) is a principal value integral with a small disk removed at $\vec{r}_s'$.

Summarizing the formulas for the pole terms for the case of first-order poles [10,12,17,18] we have for natural frequencies and modes

$$\langle \tilde{\bar{Z}}(\vec{r}_s,\vec{r}_s';s_\alpha) \cdot \vec{j}_{s_\alpha}(\vec{r}_s') \rangle = \vec{0}$$

$$s_\alpha \equiv \text{natural frequency} \tag{2.7}$$

$$\vec{j}_{s_\alpha}(\vec{r}_s') \equiv \text{natural mode}$$

In terms of the moment method [16] which matricizes such an integral equation this can be solved for the natural frequencies and modes, but this is not our concern here. Similarly the coupling vectors can be solved from

$$\langle \vec{j}_{s_\alpha}(\vec{r}_s) \cdot \tilde{\bar{Z}}(\vec{r}_s,\vec{r}_s';s_a) \rangle = \vec{0} \tag{2.8}$$

In this case where we are using the symmetric impedance kernel the coupling vector and natural mode are the same, but in general they need not be the same. We can normalize the natural modes via

$$\langle \vec{j}_{s_\alpha}(\vec{r}_s) \cdot \vec{j}_{s_\alpha}(\vec{r}_s) \rangle = 1 \tag{2.9}$$

However, other normalizations can be chosen at convenience, such as the commonly used one of setting the maximum magnitude (or some other convenient magnitude) to 1.

The coupling coefficient (class 1) is then computed from

$$\eta_\alpha = \frac{\langle \vec{j}_{s_\alpha}(\vec{r}_s) \cdot \tilde{\vec{E}}_s(\vec{r}_s, s_\alpha) \rangle}{\langle \vec{j}_{s_\alpha}(\vec{r}_s) \cdot \tilde{\bar{\bar{Z}}}_1(\vec{r}_s, \vec{r}'_s; s_\alpha) \cdot \vec{j}_{s_\alpha}(\vec{r}'_s) \rangle} \qquad (2.10)$$

$$\tilde{\bar{\bar{Z}}}_1(\vec{r}_s, \vec{r}'_s; s) = \frac{\partial}{\partial s} \tilde{\bar{\bar{Z}}}(\vec{r}, \vec{r}'; s)$$

Note that the spatial variables have all been integrated out, leaving η_α dependent only on the incident wave (or "source" field) conditions (for $s = s_\alpha$ in class 1).

III. Symmetry and SEM-Pole Parameters

As discussed in [7] the presence of an electromagnetic symmetry plane allows the natural modes to be organized into two sets according to their symmetry properties. As indicated in fig. 3.1 let there be a symmetry plane P taken as the (x,y) plane. This kind of symmetry is also referred to as reflection or mirror symmetry which has the formulas

$$\begin{aligned}
\overleftrightarrow{R} &\equiv \begin{pmatrix} 1 & 0 & 0 \\ 0 & 1 & 0 \\ 0 & 0 & -1 \end{pmatrix} \equiv \text{reflection dyad} \\
&= \overleftrightarrow{R}^{-1} \\
\vec{r} &\equiv x\vec{1}_x + y\vec{1}_y + z\vec{1}_z \equiv \text{position or coordinates} \\
\vec{r}_m &\equiv \overleftrightarrow{R} \cdot \vec{r} \equiv \text{mirror position or mirror coordinates} \\
&= x\vec{1}_x + y\vec{1}_y - z\vec{1}_z
\end{aligned} \tag{3.1}$$

For each position $\vec{r}$ at say a conductor another conductor is at $\vec{r}_m$, etc. This is readily generalized to include matrix permittivity, permeability, and conductivity [4], but the above is sufficient for present purposes. Note in fig. 3.1 the illustration is for the case of two objects symmetrical with respect to P, which will be important later. However, the general results also apply to a single (connected) object with a symmetry plane.

With respect to P the fields and surface current density can be decomposed into two parts, designated symmetric and antisymmetric, as

$$\begin{aligned}
\vec{E}_{\substack{sy \\ as}}(\vec{r},t) &= \frac{1}{2}\{\vec{E}(\vec{r},t) \pm \overleftrightarrow{R} \cdot \vec{E}(\vec{r}_m,t)\} \\
\vec{H}_{\substack{sy \\ as}}(\vec{r},t) &= \frac{1}{2}\{\vec{H}(\vec{r},t) \mp \overleftrightarrow{R} \cdot \vec{H}(\vec{r}_m,t)\}
\end{aligned} \tag{3.2}$$

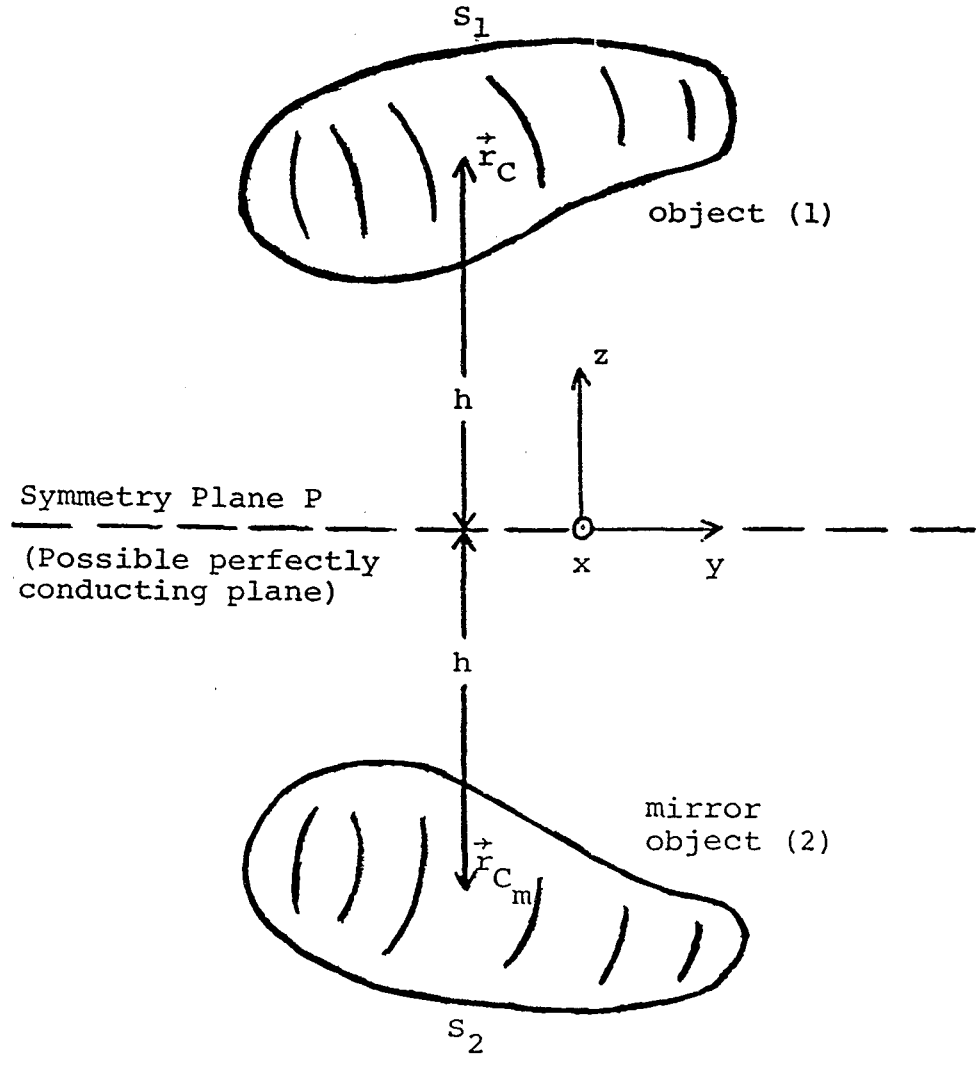

Figure 3.1 Two objects symmetrical with respect to a plane.

$$\vec{J}_{s_{\substack{sy\\as}}}(\vec{r},t) = \frac{1}{2}\{\vec{J}_s(\vec{r}_s,t) \pm \overleftrightarrow{R} \cdot \vec{J}_s(\vec{r}_{s_m},t)\}$$

where the upper sign corresponds to symmetric (subscript sy) and the lower sign to antisymmetric (subscript as). The original fields etc. can be reconstructed by merely adding symmetric and antisymmetric parts.

The surface-current-density natural modes can be divided similarly into two kinds with the property

$$\vec{j}_{s_{\substack{sy\\as},\alpha'}}(\vec{r}) = \pm \overleftrightarrow{R} \cdot \vec{j}_{s_{\substack{sy\\as},\alpha'}}(\vec{r}_m) \tag{3.3}$$

$$\alpha = (\substack{sy\\as},\alpha') = \text{natural mode index set}$$

The modes can then be constructed with the property that they each fit into one of two categories, symmetric and antisymmetric. The associated natural frequencies can then be designated by this decomposition as $s_{\substack{sy\\as},\alpha'}$. Note that not all the natural frequencies need be distinct; there can be cases of degeneracy, such as when higher order symmetries are also present.

The coupling coefficient is

$$\eta_{\substack{sy\\as},\alpha'} = \frac{\langle \vec{j}_{s_{\substack{sy\\as},\alpha'}}(\vec{r}_s) \cdot \tilde{\vec{E}}_s(\vec{r}_s, s_{\substack{sy\\as},\alpha'}) \rangle}{\langle \vec{j}_{s_{\substack{sy\\as},\alpha'}}(\vec{r}_s) \cdot \overleftrightarrow{Z}_1(\vec{r}_s,\vec{r}'_s; s_{\substack{sy\\as},\alpha'}) \cdot \vec{j}_{s_{\substack{sy\\as},\alpha'}}(\vec{r}'_s) \rangle} \tag{3.4}$$

$$= \frac{\langle \vec{j}_{s_{as}^{sy},\alpha'}(\vec{r}_s) \cdot \tilde{\vec{E}}_{s_{sy}^{as}}(\vec{r}_s, s_{as}^{sy},\alpha') \rangle}{\langle \vec{j}_{s_{as}^{sy},\alpha'}(\vec{r}_s) \cdot \tilde{\vec{Z}}_1(\vec{r}_s,\vec{r}_s';s_{as}^{sy},\alpha') \cdot \vec{j}_{s_{as}^{sy},\alpha'}(\vec{r}_s') \rangle}$$

Note here that the incident or source field also decomposes into symmetric and antisymmetric parts, each of which contributes only to its corresponding type of coupling coefficient.

IV. SEM-Pole Parameters for Two Objects Symmetrical with Respect to a Plane

Consider first that there is only one object present on one side of P and not touching P. As in fig. 3.1 designate this as object 1 with surface S_1. For later use it is convenient to define some effective center of this object as $\vec{r}_C$ so that

$$z_C = h \tag{4.1}$$

If desired one can also choose

$$(x_C, y_C) = (0,0) \tag{4.2}$$

but this is arbitrary.

Using a superscript 1 to designate SEM parameters for this case we have

$$\underset{\vec{r}_s \quad S_1}{<\tilde{\tilde{Z}}(\vec{r}_s,\vec{r}_s';s_\alpha^{(1)}) \; ; \; \vec{j}_{s_\alpha}^{(1)}(\vec{r}_s')>_1} = \vec{0} \tag{4.3}$$

where the integration ($\vec{r}_s'$ in this case) is over S_1 as designated by the subscript on the symmetric product. The coupling coefficient is now

$$\eta_\alpha^{(1)} = \frac{<\vec{j}_{s_\alpha}^{(1)}(\vec{r}_s) \; ; \; \tilde{\tilde{E}}_s(\vec{r}_s,s_\alpha^{(1)})>_1}{{}_1<\vec{j}_{s_\alpha}^{(1)}(\vec{r}_s) \; ; \; \tilde{\tilde{Z}}_1(\vec{r}_s,\vec{r}_s';s_\alpha^{(1)}) \; ; \; \vec{j}_{s_\alpha}^{(1)}(\vec{r}_s')>_1} \tag{4.4}$$

Note the introduction here of a presubscript on the symmetric product in the denominator to denote integration of the first spatial coordinates over S_1 while the postscript handles this function for the second spatial coordinates.

Now of course the symmetry in fig. 3.1 makes it arbitrary which object is labelled "1" and which "2". Then (4.3) and (4.4) can be rewritten with 1 → 2. Since the coordinates of object 1 are transformed to object 2 by the reflection dyad in (3.1) we have

$$\begin{aligned} s_\alpha^{(2)} &= s_\alpha^{(1)} \\ \vec{j}^{(2)}_{s_\alpha}(\vec{r}_s) &= \overleftrightarrow{R} \cdot \vec{j}^{(1)}_{s_\alpha}(\overleftrightarrow{R} \cdot \vec{r}_s) \\ \eta_\alpha^{(2)} &= \eta_\alpha^{(1)} \Big|_{\vec{\tilde{E}}_s(\vec{r}_s, s_\alpha^{(1)}) \to \overleftrightarrow{R} \cdot \vec{\tilde{E}}_s(\overleftrightarrow{R} \cdot \vec{r}_s, s_\alpha^{(1)})} \end{aligned} \tag{4.5}$$

Now define an unperturbed natural mode over both objects as

$$\vec{j}^{(0)}_{\substack{s_{sy} \\ as}, \alpha'}(\vec{r}_s) = \vec{j}^{(1)}_{s_{\alpha'}}(\vec{r}_s) \pm \overleftrightarrow{R} \cdot \vec{j}^{(1)}_{s_{\alpha'}}(\overleftrightarrow{R} \cdot \vec{r}_s) \tag{4.6}$$

As one can verify, this mode satisfies (4.3) with

$$s_{\alpha'}^{(0)} = s_\alpha^{(1)} = s_\alpha^{(2)} \tag{4.7}$$

provided the fields at one object from the other can be neglected. Under a similar assumption the unperturbed coupling coefficient can be computed from

$$\eta^{(0)}_{\substack{sy \\ as}, \alpha'} = \frac{\langle \vec{j}^{(1)}_{s_{\alpha'}}(\vec{r}_s) \cdot \vec{\tilde{E}}_s(\vec{r}_s, s_{\alpha'}^{(0)} \pm \overleftrightarrow{R} \cdot \vec{\tilde{E}}_s(\overleftrightarrow{R} \cdot \vec{r}_s, s_{\alpha'}^{(0)}) \rangle_1}{2 \; {}_1\langle \vec{j}^{(1)}_{s_{\alpha'}}(\vec{r}_s) \cdot \overleftrightarrow{\tilde{Z}}_1(\vec{r}_s, \vec{r}'_s; s_{\alpha'}^{(0)}) \cdot \vec{j}^{(1)}_{s_{\alpha'}}(\vec{r}'_s) \rangle_1}$$

$$= \frac{\langle \vec{j}^{(1)}_{s_{\alpha'}}(\vec{r}_s) \; ; \; \tilde{\vec{E}}_{s_{sy}}(\vec{r}_s, s^{(0)}_{\alpha'}) \rangle_1}{{}_1\langle \vec{j}^{(1)}_{s_{\alpha'}}(\vec{r}_s) \; ; \; \tilde{\vec{Z}}_1(\vec{r}_s, \vec{r}'_s; s^{(0)}_{\alpha'}) \; ; \; \vec{j}^{(1)}_{s_\alpha}(\vec{r}'_s) \rangle_1} \qquad (4.8)$$

Note that since the integration is only over object 1, then as in (4.6) it does not matter whether a symmetric or antisymmetric mode is used. Note the similarity to (4.4), except for the introduction of the symmetric and antisymmetric parts of the electric field.

The kernel (as in (2.4) and (2.6)) has some symmetry properties. Since on our object

$$R = |\vec{r}_s - \vec{r}'_s| = |\overleftrightarrow{R} \cdot (\vec{r}_s - \vec{r}'_s)| = |\vec{r}_{s_m} - \vec{r}'_{s_m}| = R_m$$

$$\vec{I}_R \vec{I}_R = \frac{(\vec{r}_s - \vec{r}'_s)(\vec{r}_s - \vec{r}'_s)}{|\vec{r}_s - \vec{r}'_s|^2}$$

$$= \frac{\overleftrightarrow{R} \cdot (\vec{r}_{s_m} - \vec{r}'_{s_m})(\vec{r}_{s_m} - \vec{r}'_{s_m}) \cdot \overleftrightarrow{R}}{|\vec{r}_{s_m} - \vec{r}'_{s_m}|^2} = \overleftrightarrow{R} \cdot \vec{I}_{R_m} \vec{I}_{R_m} \cdot \overleftrightarrow{R} \qquad (4.9)$$

$$\vec{I}_S(\vec{r}_s)\vec{I}_S(\vec{r}_s) = \overleftrightarrow{R} \cdot \vec{I}_S(\vec{r}_{s_m})\vec{I}_S(\vec{r}_{s_m}) \cdot \overleftrightarrow{R}$$

$$\vec{I}_S(\vec{r}'_s)\vec{I}_S(\vec{r}'_s) = \overleftrightarrow{R} \cdot \vec{I}_S(\vec{r}'_{s_m})\vec{I}_S(\vec{r}'_{s_m}) \cdot \overleftrightarrow{R}$$

then a complete interchange between positions and orientations between objects 1 and 2 is allowed, i.e.

$$\tilde{\vec{Z}}(\vec{r}_s, \vec{r}'_s; s) = \overleftrightarrow{R} \cdot \tilde{\vec{Z}}(\vec{r}_{s_m}, \vec{r}'_{s_m}; s) \cdot \overleftrightarrow{R} \qquad (4.10)$$

A similar result holds for $\tilde{\vec{Z}}_1$.

Applying (2.7) with operation on the left by the natural mode gives a scalar relation

$$1\cup 2\langle \vec{j}_{s_{\substack{sy\\as}},\alpha'}(\vec{r}_s)\ ;\ \tilde{\tilde{Z}}(\vec{r}_s,\vec{r}'_s;s_{\substack{sy\\as}},\alpha')\ ;\ \vec{j}_{s_{\substack{sy\\as}},\alpha'}(\vec{r}'_s)\rangle_{1\cup 2} = 0 \tag{4.11}$$

Note that integration of both $\vec{r}_s$ and $\vec{r}'_s$ is over $S_1 \cup S_2$, giving (4.11) a completely symmetrical form. We can think of the integration in (4.11) as comprising 4 terms by splitting the integration according to S_1 and S_2 separately. In short-hand form (4.10) can then be written as

$$0 = {}_1\langle\ ;\ ;\ \rangle_1 + {}_1\langle\ ;\ ;\ \rangle_2 + {}_2\langle\ ;\ ;\ \rangle_1 + {}_2\langle\ ;\ ;\ \rangle_2 \tag{4.12}$$

Next utilizing the symmetry properties of the natural modes and kernel, and changing variables by reflection from one object to the other we have

$$\begin{aligned}
&{}_2\langle \vec{j}_{s_{\substack{sy\\as}},\alpha'}(\vec{r}_s);\tilde{\tilde{Z}}(\vec{r}_s,\vec{r}'_s;s_{\substack{sy\\as}},\alpha');\vec{j}_{s_{\substack{sy\\as}},\alpha'}(\vec{r}'_s)\rangle_2 \\
&= {}_1\langle \pm\vec{j}_{s_{\substack{sy\\as}},\alpha'}(\vec{r}_s)\cdot\overleftrightarrow{R};\overleftrightarrow{R}\cdot\tilde{\tilde{Z}}(\vec{r}_s,\vec{r}'_s;s_{\substack{sy\\as}},\alpha')\cdot\overleftrightarrow{R};\pm\overleftrightarrow{R}\cdot\vec{j}_{s_{\substack{sy\\as}},a'}(\vec{r}'_s)\rangle_1 \\
&= {}_1\langle \vec{j}_{s_{\substack{sy\\as}},\alpha'}(\vec{r}_s);\tilde{\tilde{Z}}(\vec{r}_s,\vec{r}'_s;s_{\substack{sy\\as}},\alpha');j_{s_{\substack{sy\\as}},\alpha'}(\vec{r}'_s)\rangle_1
\end{aligned} \tag{4.13}$$

$$\begin{aligned}
&{}_2\langle \vec{j}_{s_{\substack{sy\\as}},\alpha'}(\vec{r}_s);\tilde{\tilde{Z}}(\vec{r}_s,\vec{r}'_s;s_{\substack{sy\\as}},\alpha');\vec{j}_{s_{\substack{sy\\as}},\alpha'}(\vec{r}'_s)\rangle_1 \\
&= {}_1\langle \pm\vec{j}_{s_{\substack{sy\\as}},\alpha'}(\vec{r}_s)\cdot\overleftrightarrow{R};\overleftrightarrow{R}\cdot\tilde{\tilde{Z}}(\vec{r}_s,\vec{r}'_s;s_{\substack{sy\\as}},\alpha')\cdot R;\pm\overleftrightarrow{R}\cdot\vec{j}_{s_{\substack{sy\\as}},a'}(\vec{r}'_s)\rangle_2 \\
&= {}_1\langle \vec{j}_{s_{\substack{sy\\as}},\alpha'}(\vec{r}_s);\tilde{\tilde{Z}}(\vec{r}_s,\vec{r}'_s;s_{\substack{sy\\as}},\alpha');\vec{j}_{s_{\substack{sy\\as}},\alpha'}(\vec{r}'_s)\rangle_2
\end{aligned}$$

Then (4.11) reduces to

$$0 = {}_1\langle \vec{j}_{s_{sy_{as},\alpha'}}(\vec{r}_s); \tilde{\vec{Z}}(\vec{r}_s,\vec{r}'_s;s_{sy_{as},\alpha'}); \vec{j}_{s_{sy_{as},\alpha'}}(\vec{r}'_s)\rangle_{1U2}$$

$$= {}_1\langle \vec{j}_{s_{sy_{as},\alpha'}}(\vec{r}_s); \tilde{\vec{Z}}(\vec{r}_s,\vec{r}'_s;s_{sy_{as},\alpha'}); \vec{j}_{s_{sy_{as},\alpha'}}(\vec{r}'_s)\rangle_1$$

$$+ {}_1\langle \vec{j}_{s_{sy_{as},\alpha'}}(\vec{r}_s); \tilde{\vec{Z}}(\vec{r}_s,\vec{r}'_s;s_{sy_{as},\alpha'}); \vec{j}_{s_{sy_{as},\alpha'}}(\vec{r}'_s)\rangle_2 \qquad (4.14)$$

This result can also be obtained from (2.7) by dot multiplication on the left by the natural mode and integration only over object 1.

The coupling coefficient formula in (3.4) similarly reduces using

$$\langle \vec{j}_{s_{sy_{as},\alpha'}}(\vec{r}_s); \tilde{\vec{E}}_{s_{sy_{as}}}(\vec{r}_s,s_{sy_{as},\alpha'})\rangle_{1U2}$$

$$= 2\langle \vec{j}_{s_{sy_{as},\alpha'}}(\vec{r}_s); \tilde{\vec{E}}_{s_{sy_{as}}}(\vec{r}_s,s_{sy_{as},\alpha'})\rangle_1 \qquad (4.15)$$

Combining this with (4.13) (using $\tilde{\vec{Z}}_1$ instead of $\tilde{\vec{Z}}$) gives

$$\eta_{sy_{as},\alpha'} = \frac{\langle \vec{j}_{s_{sy_{as},\alpha'}}(\vec{r}_s) \cdot \tilde{\vec{E}}_{s_{sy_{as}}}(\vec{r}_s,s_{sy_{as},\alpha'})\rangle_1}{{}_1\langle \vec{j}_{s_{sy_{as},\alpha'}}(\vec{r}_s) \cdot \tilde{\vec{Z}}_1(\vec{r}_s,\vec{r}'_s;s_{sy_{as},\alpha'}) \cdot \vec{j}_{s_{sy_{as},\alpha'}}(\vec{r}'_s)\rangle_{1U2}} \qquad (4.16)$$

V. Interaction of Object and Mirror Object

In (4.14) we have a term involving integration over $\vec{r}_s$ on object 1 and $\vec{r}'_s$ on object 2. As the objects are separated to larger and larger distances apart, the kernel, which is a function of $\vec{r}_s - \vec{r}'_s$, can be approximated using a far-field approximation as (for $R \to \infty$)

$$\tilde{\overleftrightarrow{Z}}(\vec{r}_s,\vec{r}'_s;s) = \tilde{\overleftrightarrow{Z}}_f(\vec{r}_s,\vec{r}'_s;s) + 0(e^{-\gamma R}R^{-2})$$

$$\tilde{\overleftrightarrow{Z}}_f(\vec{r}_s,\vec{r}'_s;s) = \frac{s\mu_0}{4\pi R} e^{-\gamma R} \overleftrightarrow{I}_t(\vec{r}_s)\cdot[\overleftrightarrow{I} - \vec{I}_R\vec{I}_R]\cdot\overleftrightarrow{I}_t(r'_s) + 0(e^{-\gamma R}R^{-2}) \tag{5.1}$$

Note the inclusion of $e^{-\gamma R}$ in the order symbols since s (and hence γ) is complex. Here

$$R = |\vec{r}_s - \vec{r}'_s| \tag{5.2}$$

Continuing the approximation note that $\vec{r}_s$ varies over object 1 and $\vec{r}'_s$ varies over object 2. In order to have some origin for these two sets of coordinates recall, as in fig. 3.1, that these two objects have some equivalent centers designated as $\vec{r}_C$ and $\vec{r}_{C_m}$, respectively. Then define

$$\begin{aligned} \vec{r}_s &\equiv \vec{r}_1 + \vec{r}_C \\ \vec{r}'_s &\equiv \vec{r}_2 + \vec{r}_{C_m} = \vec{r}_2 + \overleftrightarrow{R}\cdot\vec{r}_C \end{aligned} \tag{5.3}$$

Let

$$\ell \equiv 2h = |\vec{r}_C - \vec{r}_{C_m}| \tag{5.4}$$

and as $\ell \to \infty$ then $\vec{r}_1$ and $\vec{r}_2$ remain bounded by the linear dimensions of the object. Furthermore, setting

$$\vec{r}_C = h\vec{1}_z \ , \ \vec{r}_{C_m} = -h\vec{1}_z \tag{5.5}$$

we have

$$\begin{aligned} \vec{r}_s &= \vec{r}_1 + h\vec{1}_z \\ \vec{r}_s' &= \vec{r}_2 - h\vec{1}_z \\ \vec{r}_s - \vec{r}_s' &= \vec{r}_1 - \vec{r}_2 + \ell\vec{1}_z \end{aligned} \tag{5.6}$$

Next expand the various terms in (5.1) for large ℓ as

$$\begin{aligned} R &= \{[\vec{r}_1 - \vec{r}_2 + \ell\vec{1}_z]\cdot[\vec{r}_1 - \vec{r}_2 + \ell\vec{1}_z]\}^{\frac{1}{2}} \\ &= \ell\{1 + \frac{2}{\ell}\,\vec{1}_z\cdot[\vec{r}_1 - \vec{r}_2] + \frac{1}{\ell^2}\,(\vec{r}_1 - \vec{r}_2)\cdot(\vec{r}_1 - \vec{r}_2)\}^{\frac{1}{2}} \\ &= \ell + \vec{1}_z\cdot[\vec{r}_1 - \vec{r}_2] + 0(\ell^{-1}) \quad \text{as } \ell \to \infty \end{aligned}$$

$$\begin{aligned} \vec{1}_R &= \frac{\vec{r}_1 - \vec{r}_2 + \ell\vec{1}_z}{|\vec{r}_1 - \vec{r}_2 + \ell\vec{1}_z|} = \frac{\vec{1}_z + \dfrac{\vec{r}_1 - \vec{r}_2}{\ell}}{\left|\vec{1}_z + \dfrac{\vec{r}_1 - \vec{r}_2}{\ell}\right|} \\ &= \frac{\vec{1}_z + 0(\ell^{-1})}{1 + 0(\ell^{-1})} \\ &= \vec{1}_z + 0(\ell^{-1}) \quad \text{as } \ell \to \infty \end{aligned}$$

$$\begin{aligned} &\vec{1}_S(\vec{r}_s) \equiv \vec{1}_{S_1}(\vec{r}_1) \\ &\vec{1}_S(\vec{r}_s') \equiv \vec{1}_{S_2}(\vec{r}_2) = \overset{\leftrightarrow}{R}\cdot\vec{1}_{S_1}(\vec{r}_1) \\ &\overset{\leftrightarrow}{1}_t(\vec{r}_s) \equiv \overset{\leftrightarrow}{1}_{t_1}(\vec{r}_1) = \overset{\leftrightarrow}{1} - \vec{1}_{S_1}(\vec{r}_1)\vec{1}_{S_1}(\vec{r}_1) \end{aligned} \tag{5.7}$$

$$\overleftrightarrow{I}_t(\vec{r}_s') \equiv \overleftrightarrow{I}_{t_2}(\vec{r}_2) = \overleftrightarrow{I} - \vec{I}_{s_2}(\vec{r}_2)\vec{I}_{s_2}(\vec{r}_2) = \overleftrightarrow{R}\cdot\overleftrightarrow{I}_{t_1}(\vec{r}_1)\cdot\overleftrightarrow{R}$$

Now substitute these large ℓ approximations into 5.1 to give

$$\begin{aligned}
&\tilde{\overleftrightarrow{Z}}_f(\vec{r}_s,\vec{r}_s';s) = \tilde{\overleftrightarrow{Z}}_{f_o}(\vec{r}_1,\vec{r}_2,\ell;s) + 0(e^{-\gamma\ell}\ell^{-2}) \quad \text{as } \ell \to \infty \\
&\tilde{\overleftrightarrow{Z}}_{f_o}(\vec{r}_1,\vec{r}_2,\ell;s) = \frac{s\mu_0}{4\pi\ell}\, e^{-\gamma\ell} e^{-\gamma\vec{I}_z\cdot[\vec{r}_1-\vec{r}_2]}\overleftrightarrow{I}_{f_o}(\vec{r}_1,\vec{r}_2) \qquad (5.8) \\
&\overleftrightarrow{I}_{f_o}(\vec{r}_1,\vec{r}_2) \equiv \overleftrightarrow{I}_{t_1}(\vec{r}_1)\cdot[\overleftrightarrow{I} - \vec{I}_z\vec{I}_z]\cdot\overleftrightarrow{I}_{t_2}(\vec{r}_2) = \overleftrightarrow{R}\cdot\overleftrightarrow{I}_{f_o}(\vec{r}_2,\vec{r}_1)\cdot\overleftrightarrow{R}
\end{aligned}$$

Then we have

$$\tilde{\overleftrightarrow{Z}}(\vec{r}_s,\vec{r}_s';s) = \tilde{\overleftrightarrow{Z}}_{f_o}(\vec{r}_1,\vec{r}_2,\ell;s) + 0(e^{-\gamma\ell}\ell^{-2}) \quad \text{as } \ell \to \infty \qquad (5.9)$$

So at this point we have the leading term in the kernel as $\ell \to \infty$. One could carry out the analysis further and obtain the next term of order $e^{-\gamma\ell}\ell^{-2}$ etc. However, the complexity increases considerably.

A related question is the optimal definition of $\vec{r}_C$ as some effective center of object 1. As one varies this the higher order terms are changed considerably. Perhaps one can use these terms to define $\vec{r}_C$. For the present one can use any symmetry of object 1 (such as the center of a finite length circular cylinder) to define $\vec{r}_C$.

From (4.14) replacing the coordinates on object 1 by $\vec{r}_1$ or $\vec{r}_1'$ and on object 2 by $\vec{r}_2$ or $\vec{r}_2'$ we have

$$
\begin{aligned}
&{}_1\langle \vec{j}_{s_{\substack{sy\\as},\alpha'}}(\vec{r}_s); \tilde{\tilde{Z}}(\vec{r}_s,\vec{r}'_s;s_{\substack{sy\\as},\alpha'}); \vec{j}_{s_{\substack{sy\\as},\alpha'}}(\vec{r}'_s)\rangle_2 \\
&\quad = {}_1\langle \vec{j}_{s_{\substack{sy\\as}}}(\vec{r}_1); \tilde{\tilde{Z}}_{f_o}(\vec{r}_1,\vec{r}_2,\ell;s_{\substack{sy\\as},\alpha'}); \vec{j}_{s_{\substack{sy\\as},\alpha'}}(\vec{r}_2)\rangle_2 \\
&\qquad + 0\left(e^{-\gamma_{\substack{sy\\as},\alpha'}\ell}\ell^{-2}\right) \\
&\quad = s_{\substack{sy\\as},\alpha'}\mu_0 \frac{e^{-\gamma_{\substack{sy\\as},\alpha'}\ell}}{4\pi\ell} {}_1\langle \vec{j}_{s_{\substack{sy\\as}}}(\vec{r}_1); \\
&\qquad e^{-\gamma_{\substack{sy\\as},\alpha'}\vec{l}_z\cdot[\vec{r}_1-\vec{r}_2]} \tilde{\tilde{I}}_{f_o}(\vec{r}_1,\vec{r}_2); \vec{j}_{s_{\substack{sy\\as},\alpha'}}(\vec{r}_2)\rangle_2 \\
&\qquad + 0\left(e^{-\gamma_{\substack{sy\\as},\alpha'}\ell}\ell^{-2}\right) \quad \text{as } \ell \to \infty
\end{aligned}
\tag{5.10}
$$

$$
\gamma_{\substack{sy\\as},\alpha'} \equiv \frac{1}{c} s_{\substack{sy\\as},\alpha'}
$$

Here we have shifted our definition of the natural mode to object 1 and 2 coordinates, now taken independent of ℓ.

Changing $\vec{r}_2 \to \vec{r}'_2$ and transforming from object 2 coordinates to object 1 coordinates we have

$$
\begin{aligned}
\vec{j}_{s_{\substack{sy\\as},\alpha'}}(\vec{r}'_2) &= \pm \tilde{\tilde{R}} \cdot \vec{j}_{s_{\substack{sy\\as},\alpha'}}(\vec{r}'_1) \\
\vec{r}'_2 &= \tilde{\tilde{R}} \cdot \vec{r}'_2 \\
dS_2 &= dS_1
\end{aligned}
\tag{5.11}
$$

Then the double integral in (5.10) can be changed as

$$
{}_1\langle \vec{j}_{s_{\substack{sy\\as},\alpha'}}(\vec{r}_1); e^{-\gamma_{\substack{sy\\as},\alpha'}\vec{I}_z\cdot[\vec{r}_1-\vec{r}_2]} \overleftrightarrow{I}_{f_o}(\vec{r}_1,\vec{r}_2); \vec{j}_{s_{\substack{sy\\as},\alpha'}}(\vec{r}_2)\rangle_2
$$

$$
= \pm\, {}_1\langle \vec{j}_{s_{\substack{sy\\as},\alpha'}}(\vec{r}_1); e^{-\gamma_{\substack{sy\\as},\alpha'}\vec{I}_z\cdot[\vec{r}_1-\overleftrightarrow{R}\cdot\vec{r}_1']} \overleftrightarrow{I}_{f_o}(\vec{r}_1,\overleftrightarrow{R}\cdot\vec{r}_1');
$$

$$
\vec{j}_{s_{\substack{sy\\as},\alpha'}}(\vec{r}_1')\rangle_1 \qquad (5.12)
$$

Noting the properties of the reflection matrix the above formulas are simplified via

$$
\begin{aligned}
\overleftrightarrow{I}_{f_o}(\vec{r}_1,\overleftrightarrow{R}\cdot\vec{r}') &= \overleftrightarrow{I}_{t_1}(\vec{r}_1)\cdot[\overleftrightarrow{I}-\vec{I}_z\vec{I}_z]\cdot\overleftrightarrow{R}\cdot\overleftrightarrow{I}_{t_1}(\vec{r}_1')\cdot\overleftrightarrow{R} \\
&= \overleftrightarrow{I}_{t_1}(\vec{r}_1)\cdot[\overleftrightarrow{I}-\vec{I}_z\vec{I}_z]\cdot\overleftrightarrow{I}_{t_1}(\vec{r}') \qquad (5.13)\\
\vec{I}_z\cdot[\vec{r}_1-\overleftrightarrow{R}\cdot\vec{r}_1'] &= \vec{I}_z\cdot[\vec{r}_1+\vec{r}_1'] = [z_1+z_1']
\end{aligned}
$$

This gives

$$
{}_1\langle \vec{j}_{s_{\substack{sy\\as},\alpha'}}(\vec{r}_1); e^{-\gamma_{\substack{sy\\as},\alpha'}\vec{I}_z\cdot[\vec{r}_1-\vec{r}_2]} \overleftrightarrow{I}_{f_o}(\vec{r}_1,\vec{r}_2); \vec{j}_{s_{\substack{sy\\as},\alpha'}}(\vec{r}_2)\rangle_2
$$

$$= \pm \, {}_1\langle \vec{J}_{\substack{sy \\ as,\alpha'}}(\vec{r}_1); e^{-\gamma_{\substack{sy \\ as,\alpha'}} \vec{I}_z \cdot [\vec{r}_1 + \vec{r}_1']} \overleftrightarrow{I}_{t_1}(\vec{r}_1) \cdot$$

$$[\overleftrightarrow{I} - \vec{I}_z \vec{I}_z] \cdot \overleftrightarrow{I}_{t_1}(\vec{r}_1'); \vec{J}_{\substack{sy \\ as,\alpha'}}(\vec{r}_1')\rangle_1 \qquad (5.14)$$

So the double integral over S_1 and S_2 has been converted to a double integral over S_1 (i.e. object 1).

Note in (5.14) that only the x and y components of the tangential parts of the natural modes appear. However, the natural modes are tangential, further reducing the formula. So only the x and y components of the natural modes count. The natural frequency enters in a factor involving the z component of $\vec{r}_1 + \vec{r}_1'$, i.e. $z_1 + z_1'$. This exponential term is like a generalized phase factor over object 1 with its mirror object 2. Note that the large exponential factor involving ℓ has already been pulled out of the double integral in (5.10).

Defining

$$\overleftrightarrow{I}_{t_z} \equiv \overleftrightarrow{I} - \vec{I}_z \vec{I}_z = \vec{I}_x \vec{I}_x + \vec{I}_y \vec{I}_y \qquad (5.15)$$

then (4.14) is reduced to

$$0 = {}_1\langle \vec{J}_{\substack{sy \\ as,\alpha'}}(\vec{r}_1); \tilde{\overleftrightarrow{Z}}(\vec{r}_1, \vec{r}_1'; s_{\substack{sy \\ as,\alpha'}}); \vec{J}_{\substack{sy \\ as,\alpha'}}(\vec{r}_1')\rangle_1$$

$$\pm s_{\substack{sy \\ as,\alpha'}} \mu_0 \frac{e^{-\gamma_{\substack{sy \\ as,\alpha'}} \ell}}{4\pi\ell} {}_1\langle \vec{J}_{\substack{sy \\ as,\alpha'}}(\vec{r}_1); e^{-\gamma_{\substack{sy \\ as,\alpha'}} [z_1 + z_1']} \overleftrightarrow{I}_{t_z};$$

$$\vec{J}_{s_{sy}}(\vec{r}_1')>_1 + 0(e^{-\gamma_{sy}\ell}\ell^{-2}) \quad \text{as } \ell \to \infty \tag{5.16}$$

Well, now all integration is over only local coordinates on object 1 and the ℓ dependence is a separate factor. If desired the terms in (5.16) can now be written as

$$0 = {}_1\langle\vec{J}_{s_{sy}}(\vec{r}_1);$$

$$\tilde{\tilde{Z}}(\vec{r}_1,\vec{r}_1';s_{sy}) \pm s_{sy}\mu_0 \frac{e^{-\gamma_{sy}\ell}}{4\pi\ell} e^{-\gamma_{sy}[z_1+z_1']} \overleftrightarrow{I}_{t_z}$$

$$+ 0(e^{-\gamma_{sy}\ell}\ell^{-2})$$

$$;\vec{J}_{s_{sy}}(\vec{r}_1')>_1 \tag{5.17}$$

where now we have one double integral with various interesting terms combined in the single kernel.

VI. Perturbation Theory

At this point let us borrow some concepts from perturbation theory which is often used in quantum mechanics [13,15]. While here our derivations are for symmetric kernels they can be readily generalized to other kinds found in integral equations of electromagnetic scattering.

Consider two kernels $\overleftrightarrow{\Gamma}(\vec{r},\vec{r}')$ and $\overleftrightarrow{\Lambda}(\vec{r},\vec{r}')$ where the second is small in some sense compared to the first. The first defines vector modes according to

$$\begin{aligned} &\langle \overleftrightarrow{\Gamma}(\vec{r},\vec{r}') \,;\, \vec{j}_0(\vec{r}') \rangle = \vec{0} \\ &\langle \vec{j}_0(\vec{r}) \,;\, \overleftrightarrow{\Gamma}(\vec{r},\vec{r}') \langle = \vec{0} \end{aligned} \tag{6.1}$$

so, of course, we have assumed that $\overleftrightarrow{\Gamma}$ is singular (and will correspond to an unperturbed natural frequency while $\vec{j}_0$ corresponds to an unperturbed natural mode). We also have

$$\langle \vec{j}_0(\vec{r}) \,;\, \overleftrightarrow{\Gamma}(\vec{r},\vec{r}') \,;\, \vec{j}_0(\vec{r}') \rangle = 0 \tag{6.2}$$

Now let $\overleftrightarrow{\Lambda}$ be a perturbation kernel (also symmetric) and form the problem

$$\langle \vec{j}(\vec{r}) \,;\, \overleftrightarrow{\Gamma}(\vec{r},\vec{r}') + p\overleftrightarrow{\Lambda}(\vec{r},\vec{r}') \,;\, \vec{j}(\vec{r}) \rangle = 0 \tag{6.3}$$

where p is the perturbation parameter and

$$p = \begin{cases} 0 \Rightarrow \text{unperturbed problem} \\ 1 \Rightarrow \text{perturbed problem} \end{cases} \tag{6.4}$$

Now expand the vector mode as a power series in p as

$$\vec{j}(\vec{r}) = \sum_{n=0}^{\infty} \vec{j}_n(\vec{r})p^n \qquad (6.5)$$

effectively assuming that $\vec{j}$ is an analytic function of p for sufficiently small p. Note that we have assumed that the unperturbed natural mode $\vec{j}_0$ is not degenerate, i.e. that there is only one natural mode satisfying (6.1) (except for an arbitrary multiplicative constant).

Substituting (6.5) in (6.3) and collecting by powers we have for n = 0 merely (6.2), i.e. nothing new. For n = 1 we have

$$\langle \vec{j}_0(\vec{r}); \overleftrightarrow{\Gamma}(\vec{r},\vec{r}'); \vec{j}_1(\vec{r}') \rangle + \langle \vec{j}_0(\vec{r}); \overleftrightarrow{\lambda}(\vec{r},\vec{r}'); \vec{j}_0(\vec{r}') \rangle + \langle \vec{j}_1(\vec{r}); \overleftrightarrow{\Gamma}(\vec{r},\vec{r}'); \vec{j}_0(\vec{r}') \rangle = 0 \qquad (6.6)$$

By (6.1) the first and third terms are zero, giving

$$\langle \vec{j}_0(\vec{r}) \; ; \; \overleftrightarrow{\lambda}(\vec{r},\vec{r}') \; ; \; \vec{j}_0(\vec{r}) \rangle = 0 \qquad (6.7)$$

So $\overleftrightarrow{\lambda}$ now has a constraint which is our basic perturbation formula.

VII. Perturbation of Natural Frequencies

Expand the kernel $\tilde{\tilde{Z}}$ near the unperturbed natural frequency as

$$\tilde{\tilde{Z}}(\vec{r}_1,\vec{r}_1';s_{\substack{sy\\as},\alpha'}) = \sum_{m=0}^{\infty} \tilde{\tilde{Z}}_n(\vec{r}_1,\vec{r}_1')(\Delta s_{\substack{sy\\as},\alpha'})^m$$

$$= \tilde{\tilde{Z}}(\vec{r}_1,\vec{r}_1';s_{\alpha'}) + \tilde{\tilde{Z}}_1(\vec{r}_1,\vec{r}_1')\Delta s_{\substack{sy\\as},\alpha'}$$

$$+ 0((\Delta s_{\substack{sy\\as},\alpha'})^2) \quad \text{as } \Delta s_{\substack{sy\\as},\alpha'} \to 0$$

$$\tilde{\tilde{Z}}_1(\vec{r}_1,\vec{r}_1') = [\frac{\partial}{\partial s}\tilde{\tilde{Z}}(\vec{r}_1,\vec{r}_1';s)]\Big|_{s=s_{\alpha'}} \tag{7.1}$$

$$s_{\substack{sy\\as},\alpha'} \equiv s_{\alpha'} + \Delta s_{\substack{sy\\as},\alpha'}$$

Note that the unperturbed natural frequency $s_{\alpha'}$ is only for object 1 in the absence of object 2 so that it is not distinguished as symmetric or antisymmetric.

Now identify $\tilde{\tilde{\Gamma}} + \tilde{\tilde{\Lambda}}$ in section VI with the kernel in (5.17) with $\tilde{\tilde{Z}}$ expanded as in (7.1) giving

$$\tilde{\tilde{\Gamma}}(\vec{r}_1,\vec{r}_1') = \tilde{\tilde{Z}}(\vec{r}_1,\vec{r}_1';s_{\alpha'})$$

$$\equiv \text{unperturbed kernel} \tag{7.2}$$

$$\tilde{\tilde{\Lambda}}(\vec{r}_1,\vec{r}_1') = \tilde{\tilde{Z}}_1(\vec{r}_1,\vec{r}_1')\Delta s_{\substack{sy\\as},\alpha'} + 0((\Delta s_{\substack{sy\\as},\alpha'}))$$

$$\pm s_{\alpha'}\mu_0 \frac{e^{-\gamma_{\alpha'}\ell}}{4\pi\ell} e^{-\gamma_{\alpha'}[z_1+z_1']}\tilde{\tilde{I}}_{t_z}[1 + 0(\Delta s_{\substack{sy\\as},\alpha'})]$$

$$+ 0(e^{-\gamma_{\alpha'}\ell}\ell^{-2}[1 + 0(\Delta s_{\substack{sy\\as},\alpha'})])$$

Looking at these order symbols we need both small Δs and small $e^{-\gamma_{\alpha'}\ell}\ell^{-2}$. However as $\ell \to \infty$ the latter eventually blows up for the general (and interesting) case that $Re[s_{\alpha'}]$ is negative. What is required is that this term be small, and this occurs for intermediate ℓ. Let us return to this later and for the moment assume $\overleftrightarrow{\Lambda}$ is small and write as an approximation

$$\overleftrightarrow{\Lambda}(\vec{r}_1,\vec{r}_1') \simeq \overleftrightarrow{Z}_1(\vec{r}_1,\vec{r}_1')\Delta s_{\substack{sy \\ as},\alpha'} \pm s_{\alpha'}\mu_0 \frac{e^{-\gamma_{\alpha'}\ell}}{4\pi\ell} e^{-\gamma_{\alpha'}[z_1+z_1']}\overleftrightarrow{I}_{t_z} \qquad (7.3)$$

The smallness of this term depends on the smallness of both Δs and $e^{-\gamma_{\alpha'}\ell}\ell^{-1}$.

Inserting (7.3) in (6.7) and rearranging terms gives

$$\Delta s_{\substack{sy \\ as},\alpha'} \simeq \mp s_{\alpha'}\mu_0 \frac{e^{-\gamma_{\alpha'}\ell}}{4\pi\ell} \frac{{}_1\langle \vec{j}_{s_{\alpha'}}(\vec{r}_1); e^{-\gamma_{\alpha'}[z_1+z_1']}\overleftrightarrow{I}_{t_z}; \vec{j}_{s_{\alpha'}}(\vec{r}_1')\rangle_1}{{}_1\langle \vec{j}_{s_{\alpha'}}(\vec{r}_1); \overleftrightarrow{Z}_1(\vec{r}_1,\vec{r}_1'); \vec{j}_{s_{\alpha'}}(\vec{r}_1')\rangle_1} \qquad (7.4)$$

Note that smallness of Δs is then assured if $e^{-\gamma_{\alpha'}\ell}\ell^{-1}$ is sufficiently small, so their smallness goes together. For convenience define

$$\nu_{\alpha'} \equiv \frac{{}_1\langle \vec{j}_{s_{\alpha'}}(\vec{r}_1); e^{-\gamma_{\alpha'}[z_1+z_1']}\overleftrightarrow{I}_{t_z}; \vec{j}_{s_{\alpha'}}(\vec{r}_1')\rangle_1}{{}_1\langle \vec{j}_{s_{\alpha'}}(\vec{r}_1); \overleftrightarrow{Z}_1(\vec{r}_1,\vec{r}_1'); \vec{j}_{s_{\alpha'}}(\vec{r}_1')\rangle_1} \qquad (7.5)$$

$\equiv$ image coefficient

Our result then takes the form

$$\Delta s_{\substack{sy \\ as},\alpha'} \simeq \mp\, s_{\alpha'}\mu_0 \frac{e^{-\gamma_{\alpha'}\ell}}{4\pi\ell}\, \nu_{\alpha'} \tag{7.6}$$

Note that $\nu_{\alpha'}$ is not a function of ℓ, the separation between centers of objects 1 and 2. It is a function of only the orientation of object 1 with respect to the symmetry plane as expressed in the numerator kernel and domain of integration. As the magnitude of $\nu_{\alpha'}$ varies, the size (or "radius") of the spiral-like curves in the s plane formed by variation of ℓ (as a parameter) also changes. The period of this spiral wrapping around $s_{\alpha'}$ is given by a change of 2π in $\mathrm{Im}[\gamma_{\alpha'}]\ell$. As one looks at natural frequencies with larger and larger imaginary parts the spiralling becomes more and more rapid.

Look now at the condition that Δs be small. Since a natural frequency should not enter into the right half of the s plane then we require (for passivity) that

$$\mathrm{Re}[\Delta s_{\substack{sy \\ as},\alpha'}] \leq -\mathrm{Re}[s_{\alpha'}] \tag{7.7}$$

Consider

$$|\Delta s_{\substack{sy \\ as},\alpha'}| \simeq |s_{\alpha'}|\mu_0|\nu_{\alpha'}| \frac{e^{-\mathrm{Re}[\gamma'_\alpha]\ell}}{4\pi\ell} \tag{7.8}$$

As ℓ is varied this has a minimum at

$$0 = \left\{\frac{d}{d\ell}\left[\frac{e^{-\mathrm{Re}[\gamma_{\alpha'}]\ell}}{\ell}\right]\right\}\Bigg|_{\ell=\ell_{min}}$$

$$= e^{-\mathrm{Re}[\gamma_{\alpha'}]\ell}\left[\frac{-\mathrm{Re}[\gamma_{\alpha'}]}{\ell} - \frac{1}{\ell^2}\right]\Bigg|_{\ell=\ell_{min}} \qquad (7.9)$$

$$-\mathrm{Re}[\gamma_{\alpha'}]\ell_{min} = 1$$

At this value the minimum shift in the natural frequency is

$$\left|\Delta s_{\substack{sy \\ as}, \alpha'}\right|_{min} \simeq -\mathrm{Re}[s_{\alpha'}]|s_{\alpha'}|\frac{\mu_0}{c}|\nu_{\alpha'}|\frac{1}{4\pi e} \qquad (7.10)$$

So for this perturbation solution to have some range of validity for ℓ around ℓ_{min} it is necessary that (7.10) give a sufficiently small natural-frequency perturbation.

As $\ell \to 0$ note that Δs blows up and (7.8) does not apply. Similarly as $\ell \to \infty$ the exponential term makes Δs blow up and (7.8) does not apply. Of course one can return to (4.14), as an exact expression, and transform the integration over object 2 to object 1 via the reflection matrix. This can be solved numerically but it does not give the simple physical insight as in (7.6).

Comparing these results to numerical results one can note the general agreement [2,3,6,9,11]. Specifically note that there is the spiral behavior for intermediate ℓ. Furthermore for both small and larger ℓ the trajectories in the s plane deviate from this behavior considerably. Note as ℓ increases the spiral is inward to a minimum radius, and then the spiral is outward.

A special case in which (7.6) does not apply is that for which $\nu_{\alpha'}$ is zero. Such a case can arise if the natural mode

vector has only z-directed currents since in (7.5) only x and y components contribute to the numerator double integral. An example of such a case is a thin wire oriented parallel to the z axis. In such a case one can return to the procedures in section V and expand to higher order in R and ℓ. One should obtain a result similar to (7.6), except one that involves larger powers of ℓ in the denominator. Some related numerical results are contained in [1], and a specific numerical example is presented in the next section.

VIII. A Numerical Example

As a specific illustration of the ideas, concepts, and relationships proffered in the previous sections, a simple numerical example is presented which evaluates several of the parameters arising from this perturbation solution approach. In particular, the s-plane trajectories of the dominant mode (half-wavelength) resonance of a thin, straight wire scatterer in the presence of its mirror image are presented and discussed. (As was discussed in an earlier section, for a pair of mirror image scatterers, the interactions may be decomposed into symmetric and antisymmetric parts. If the mirror image results from the presence of a scatterer near a perfectly conducting image plane, the scattering solution may be represented by the antisymmetric part only.)

Suppose the objects of fig. 3.1 become two straight, thin wire mirror image scatterers each of total length, L, and radius, a, with its respective center at $z = \pm h$, and the wire axis making an angle of ϕ with respect to the plane of symmetry (image plane) as shown in fig. 8.1. According to the development of section VI, the shift in the location of the natural frequency from the case of an isolated scatterer to the case of a pair of mirror-image scatterers is given by (7.4). As indicated symbolically in (7.4), this calculation requires the determination of the isolated natural frequency ($s_{\alpha'}$), the associated natural mode ($\vec{J}_{s_{\alpha'}}$), and the associated residue matrix ($\overleftrightarrow{Z}_1$), as well as the separation of the mirror-image scatterer centers (2h) and the scatterer orientation with respect to the plane of symmetry (ϕ).

An interesting issue to initiate these calculations and ruminations concerning specific values and interpretation of these perturbation parameters is the determination of the "so-called" image coefficient ($\nu_{\alpha'}$) as defined by (7.5). This form of $\nu_{\alpha'}$ is its continuous or analytical definition. It has been determined that a numerical definition of $\nu_{\alpha'}$ converges (rather nicely) to a fixed value which depends significantly on the

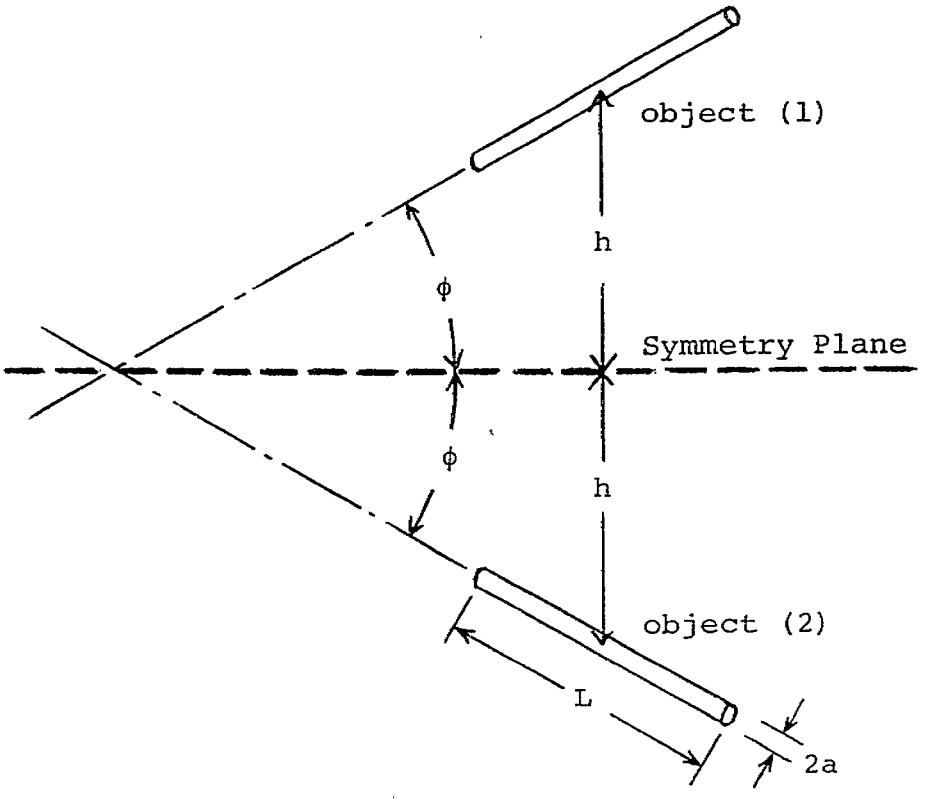

Figure 8.1 Two thin wire scatterers with a plane of symmetry.

appropriate geometrical and electrical descriptions of the mirror-image scatterers and insignificantly on the specific details of the numerical techniques utilized to arrive at its fixed value. The $\nu_{1,1}$ (along with the accompanying $s_{1,1}L/c = \gamma_{1,1}L$) is given in table 8.1 for the dominant mode pole (subscripts indicate ordering and layering [9] of singularity in the s-plane) of a straight thin wire scatterer parallel to its image plane for three different ratios of wire length to wire radius as the number of Moment Method subsectional zones is increased from 10 to 100. As was expected, the value of the image coefficient converges to a fixed value as the accuracy of the numerical solution increases. One might consider that the values of $\nu_{1,1}$ for a large number of subsectional zones should be very close to the "true" analytical value of $\nu_{1,1}$. A secondary point of interest is to note that the value of $\nu_{1,1}$ varies approximately with the inverse of the scatterer shape parameter, $2\ell n(L/a)$. This simple relationship permits one to determine a value for $\nu_{1,1}$ for some specific value of L/a, and then for "thinner" or "thicker" scatterers a good estimate of $\nu_{1,1}$ could be obtained using the simple logarithmic scale factor.

As a measure of just how well the perturbation expression of (7.4) predicts the natural frequency shifts from the isolated case in the s-plane, a direct comparison of the trajectories as predicted by the perturbation expressions and the trajectories as generated from the coupled integral equation solutions are presented in figs. 8.2-8.9. These data present the $(\gamma_{1,1})_{\substack{sy \\ as}}L$ (dominant mode symmetric and antisymmetric poles) for two parallel, straight, thin wire scatterers of four different length-to-radius ratios (L/a = 200, 400, 800, and 1600, respectively) with the scatterers' center-to-center separation/length (2h/L) varying. The "$*$" near the center of each of these spiraling trajectories represents the location of the dominant mode (half-wavelength) pole for the isolated single scatterer (or unperturbed scatterer) with the appropriate (L/a) as determined

by the integral equation solution. In section VI, an expression was given, (7.10), which predicts a minimum $\Delta s_{\substack{sy \\ as}, \alpha'}$ which occurs at a particular object-mirror object spacing, ℓ_{min}. this spiral-in, spiral-out behavior in the s-plane, seen most clearly for the "thinnest" wire in figs. 8.8 and 8.9, has been observed, questioned, and generally discussed since it was first presented in the integral equation solutions over fourteen years ago [2]. These perturbational results provide quantitative support and give additional insight into the nature of the complex natural frequencies of scattering objects in the presence of other objects.

An additional set of trajectories, figs. 8.10 and 8.11 present similar trajectories (perturbation and two-object integral equation) of $(\gamma_{1,1})_{\substack{sy \\ as}} L$ for thin, straight, mirror-image wire scatterers each making an angle of ϕ with respect to the symmetry plane. Table 8.2 presents the calculated values of the image coefficient, $\nu_{1,1}$, for L/a = 200 and 20 subsectional zones as the orientation angle, ϕ, is varied from 0° (parallel scatterers) to 90° (collinear scatterers). Again one may observe an interesting (and simple) functional variation of $\nu_{1,1}$ with ϕ. The value of $\nu_{1,1}$ appears to fall off approximately as $\cos^2(\phi)$. This follows from the comment made in section V that the mode vector which is to be used in (7.4) should be the tangential (to the symmetry plane) component of the actual isolated scatterer mode vector. Since this tangentially-projected mode vector is both pre-multiplied and post-multiplied in (7.4), it follows that the $\nu_{1,1}$ should decrease as $\cos^2(\phi)$ for increasing ϕ from 0° to 90°. This same consideration readily accounts for the fact that $\nu_{1,1}$ vanishes for two collinear thin wire scatterers (only the first order perturbational solution predicts no frequency shift; the actual integral equation solution yields small but nonzero spiraling trajectories for collinear wire scatterers of finite radius).

A final table will conclude the data representing example calculations utilizing these perturbation expansions and expressions. Table 8.3 presents the $\nu_{1,2}$, $\nu_{1,3}$, and $\nu_{1,4}$ for the first layer poles, $\gamma_{1,2}L$, $\gamma_{1,3}L$, and $\gamma_{1,4}L$, respectively, for a thin, straight wire scatterer (L/a = 200 and 20 subsectional zones) with its mirror image each making an angle of ϕ with respect to the plane of symmetry. Note that $\nu_{1,2}$ and $\nu_{1,4}$ vanish for the case when the scatterers are parallel. This situation holds for all of the ν_α, for the parallel case in which the modal distribution is an odd function about the center of the scatterer. These particular modal distributions correspond to the symmetric case as designated in previous notes [4,7]. The perturbation solution obtained in (7.4) predicts no frequency shift for these cases. Since the integral equation solution [2] indicates that a nonzero shift is incorrect, it is suggested that perturbation expansions in higher order terms of $(e^{-\gamma\ell}/\ell)$ might yield nonzero estimates of the frequency shifts in these special cases. Note that for the nonparallel cases, the $\nu_{1,2}$ and $\nu_{1,4}$ are determined with the first order perturbational expressions.

IX. Some Observations

Having obtained the perturbation of the natural frequencies by the presence of the mirror object one could go on to consider the perturbation of the natural modes. In classical perturbation theory the mode is expanded in a set of orthonormal modes [14]. In general the natural modes do not form such a set [7]. However, one can form such a set as the eigenmodes of the integral-equation kernel [5,10,18]. These can in turn be evaluated at a particular natural frequency s_α, and used for this purpose. However, this requires the computation of this (in general infinite) set of modes which may be rather laborious.

Note in (7.6) that there are two results, one for symmetric modes (minus sign) and another for antisymmetric modes (plus sign). The case of a scatterer in proximity to a perfectly conducting ground plane uses the antisymmetric results.

In a more general sense the results of (7.6), when applied to two objects symmetrical with respect to a plane as in fig. 3.1, shows that a single natural frequency is split into two distinct natural frequencies. This situation is analogous to the splitting of energy levels in quantum mechanics when two identical atoms form a diatomic molecule. A special example of this type is the hydrogen molecule ion [13]. Note, however, that energy levels in such calculations are normally real valued, while in the electromagnetic scattering problem the natural frequencies are complex valued.

References

1. L. Marin, Natural Modes of Two Collinear Cylinders, Sensor and Simulation Note 176, May 1973.

2. T. H. Shumpert, EMP Interaction With a Thin Cylinder Above a Ground Plane Using the Singularity Expansion Method, Sensor and Simulation Note 182, June 1973.

3. T. H. Shumpert and D. J. Galloway, Transient Analysis of a Finite Length Cylindrical Scatterer Very Near a Perfectly Conducting Ground, Sensor and Simulation Note 226, August 1976.

4. C. E. Baum, Interaction of Electromagnetic Fields With an Object Which Has an Electromagnetic Symmetry Plane, Interaction Note 63, March 1971.

5. C. E. Baum, On the Eigenmode Expansion Method for Electromagnetic Scattering and Antenna Problems, Part I: Some Basic Relations for Eigenmode Expansions and Their Relation to the Singularity Expansion, Interaction Note 229, January 1975.

6. K. R. Umashankar and D. R. Wilton, Transient Scattering by a Thin Wire in Free Space and Above Ground Plane Using the Singularity Expansion Method, Interaction Note 236, August 1974.

7. C. E. Baum, A Priori Application of Results of Electromagnetic Theory to the Analysis of Electromagnetic Interaction Data, Interaction Note 444, February 1985. Also in Radio Science, Vol. 22, No. 6, November-December 1987 (to appear).

8. A. D. Yaghjian, Electric Dyadic Green's Functions in the Source Region, IEEE Proc., 1980, pp. 248-263.

9. K. R. Umashankar, T. H. Shumpert, and D. R. Wilton, Scattering by a Thin Wire Parallel to a Ground Plane Using the Singularity Expansion Method, IEEE Trans. Antennas and Propagation, March 1975, pp. 178-184.

10. C. E. Baum, Emerging Technology for Transient and Broadband Analysis and Synthesis of Antennas and Scatterers, Interaction Note 300, November 1976, and IEEE Proc., November 1976, pp. 1598-1616.

11. T. H. Shumpert and D. J. Galloway, Finite Length Cylindrical Scatterer Near Perfectly Conducting Ground--A Transmission Line Mode Approximation, IEEE Trans. Antennas and Propagation, January 1978, pp. 145-151.

12. C. E. Baum, The Singularity Expansion Method: Background and Developments, Electromagnetics, 1981, pp. 351-360.

13. R. B. Leighton, Principles of Modern Physics, McGraw Hill, New York, 1959.

14. J. Mathews and R. L. Walker, Mathematical Methods of Physics, W. A. Benjamin, New York, 1965.

15. A. Messiah, Quantum Mechanics, vol. II, North-Holland Publishing Co., Amsterdam, 1966.

16. R. F. Harrington, Field Computation by Moment Methods, Macmillan, 1968.

17. C. E. Baum, The Singularity Expansion Method, in L. B. Felsen (ed.), Transient Electromagnetic Fields, Springer Verlag, 1976.

18. C. E. Baum, Toward an Engineering Theory of Electromagnetic Scattering: The Singularity and Eigenmode Expansion Methods, in P. L. E. Uslenghi (ed.), Electromagnetic Scattering, Academic Press, 1978.

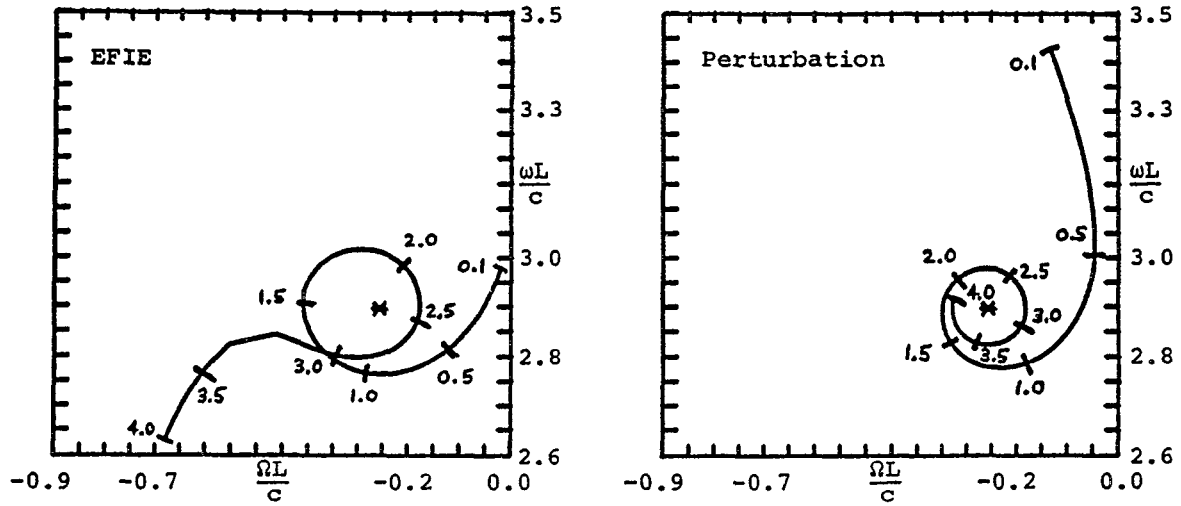

Figure 8.2 Trajectories of $\gamma_{as,1,1}L$ vs 2h/L for two parallel, thin wire scatterers with L/a = 200. (2h/L varies from 0.1 to 4.0, "✱" indicates location of natural frequency for isolated thin wire scatterer.)

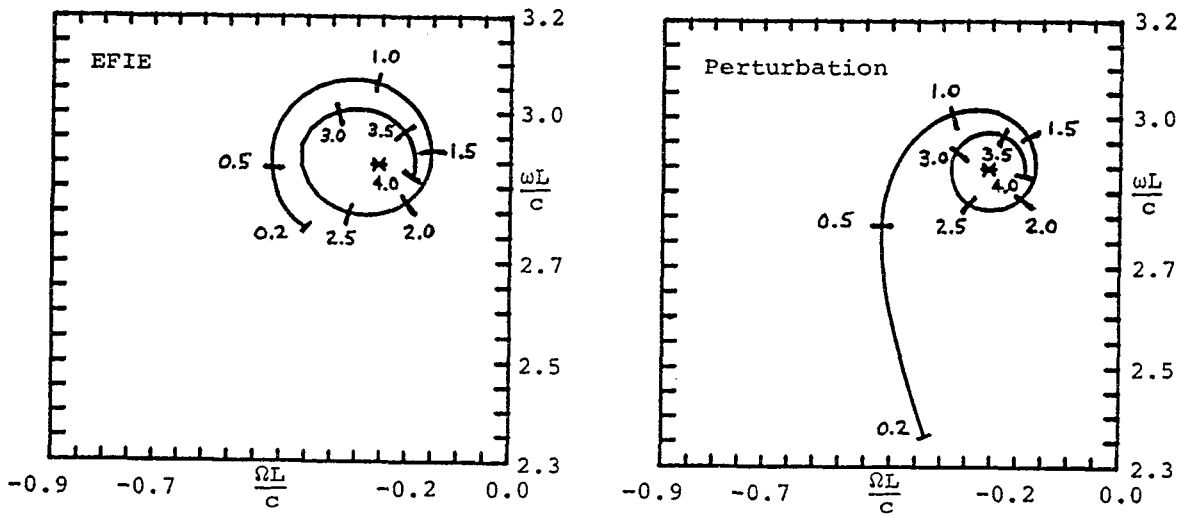

Figure 8.3 Trajectories of $\gamma_{sy,1,1}L$ vs 2h/L for two parallel, thin wire scatterers with L/a = 200. (2h/L varies from 0.2 to 4.0, "✱" indicates location of natural frequency for isolated thin wire scatterer.)

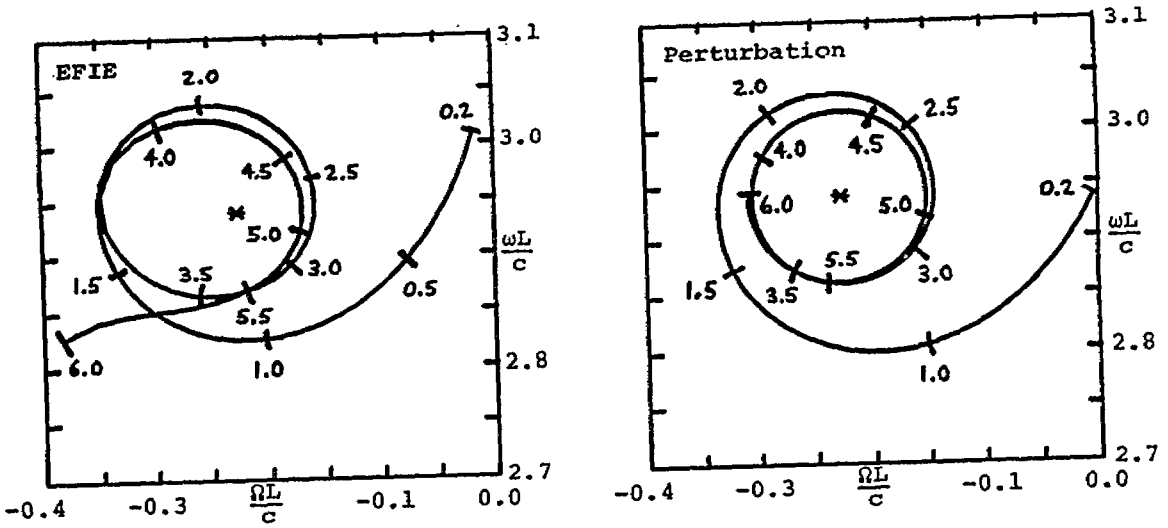

Figure 8.4 Trajectories of $\gamma_{as,1,1}L$ vs 2h/L for two parallel, thin wire scatterers with L/a = 400. (2h/L varies from 0.2 to 6.0, "✱" indicates location of natural frequency for isolated thin wire scatterer.)

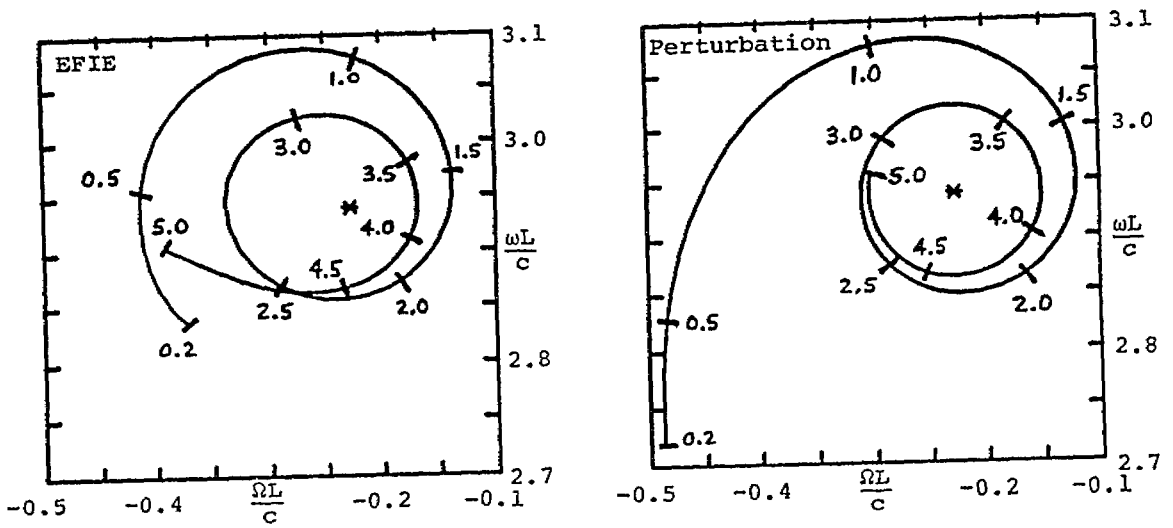

Figure 8.5 Trajectories of $\gamma_{sy,1,1}L$ vs 2h/L for two parallel, thin wire scatterers with L/a = 400. (2h/L varies from 0.2 to 5.0, "✱" indicates location of natural frequency for isolated thin wire scatterer.)

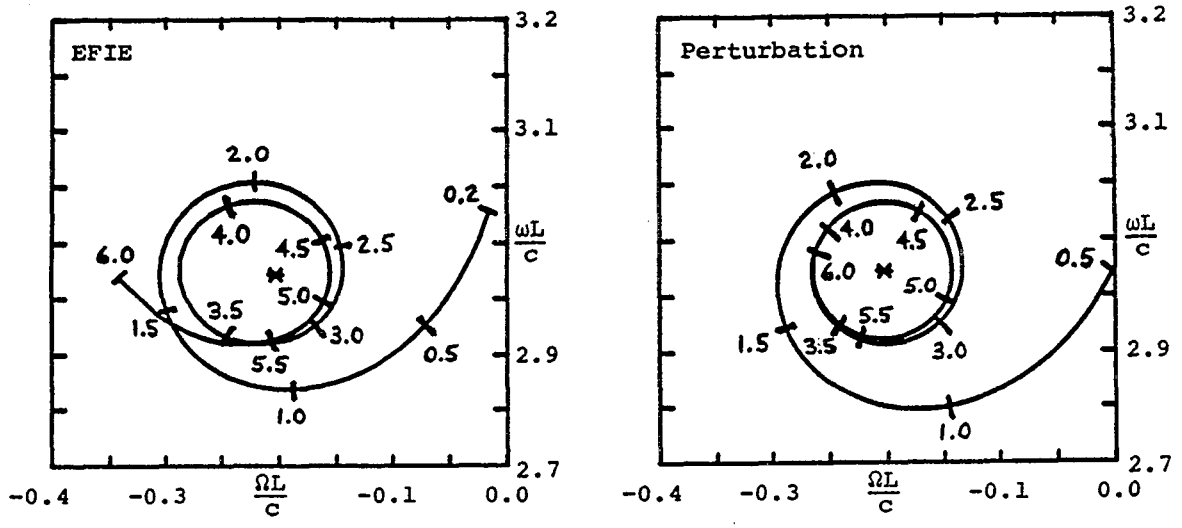

Figure 8.6 Trajectories of $\gamma_{as,1,1}L$ vs 2h/L for two parallel, thin wire scatterers with L/a = 800. (2h/L varies from 0.2 to 6.0, "✱" indicates location of natural frequency for isolated thin wire scatterer.)

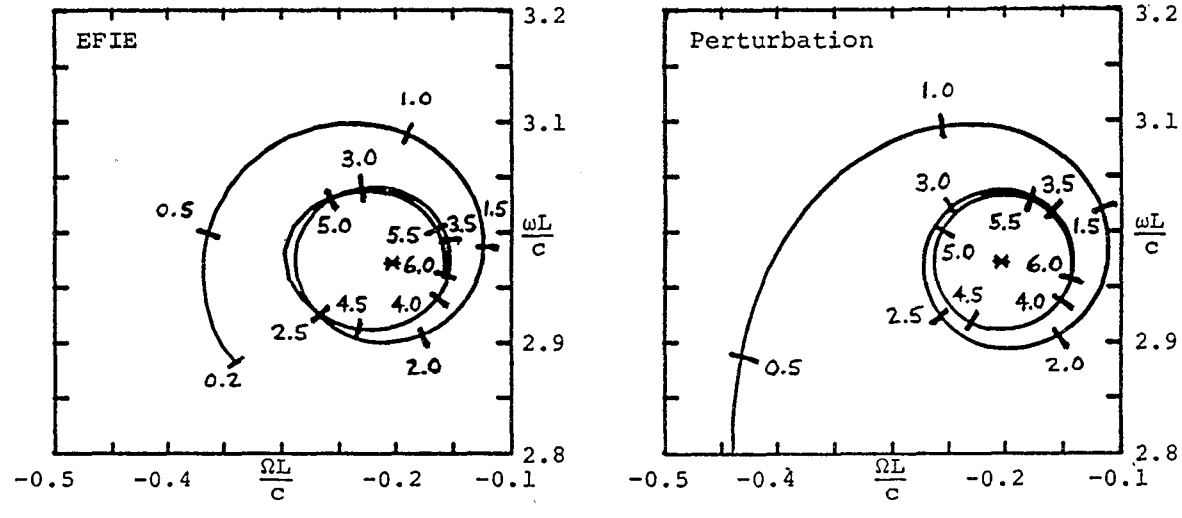

Figure 8.7 Trajectories of $\gamma_{sy,1,1}L$ vs 2h/L for two parallel, thin wire scatterers with L/a = 800. (2h/L varies from 0.2 to 6.0, "✱" indicates location of natural frequency for isolated thin wire scatterer.)

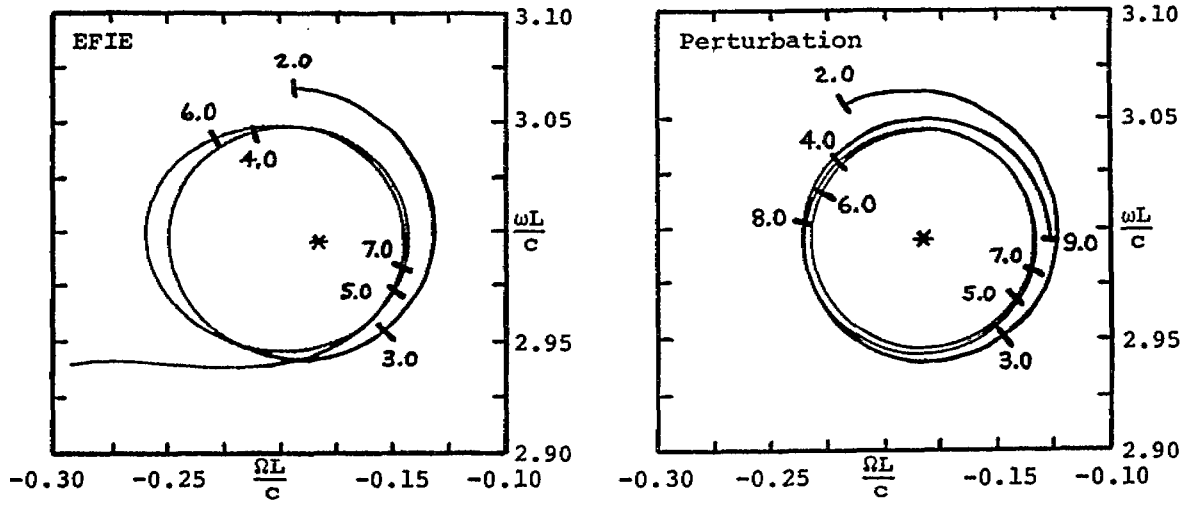

Figure 8.8 Trajectories of $\gamma_{as,1,1}L$ vs 2h/L for two parallel, thin wire scatterers with L/a = 1600. (2h/L varies from 2.0 to 9.0, "$*$" indicates location of natural frequency for isolated thin wire scatterer.)

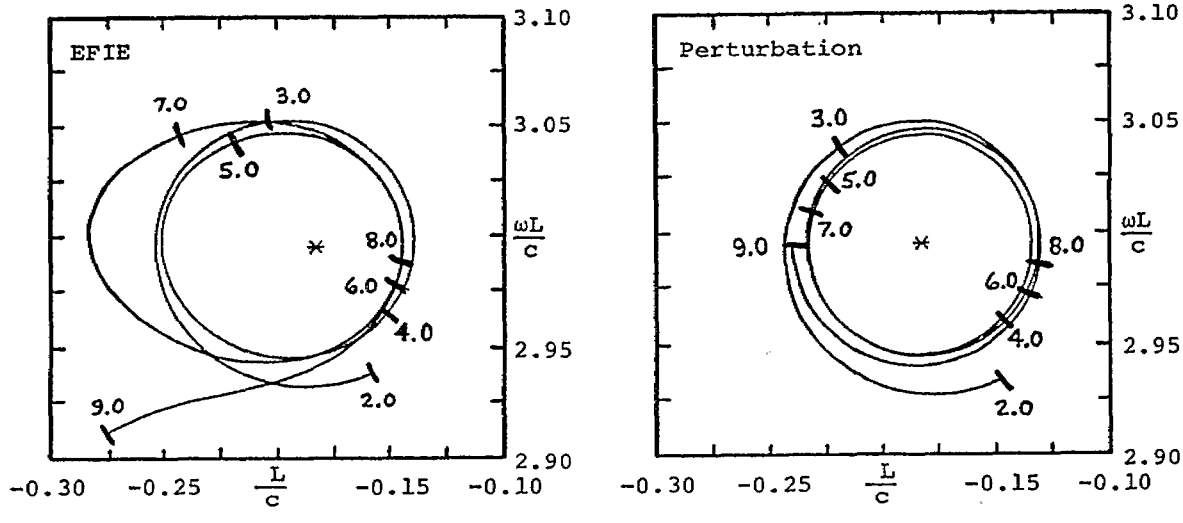

Figure 8.9 Trajectories of $\gamma_{sy,1,1}L$ vs 2h/L for two parallel, thin wire scatterers with L/a = 1600. (2h/L varies from 2.0 to 9.0, "$*$" indicates location of natural frequency for isolated thin wire scatterer.)

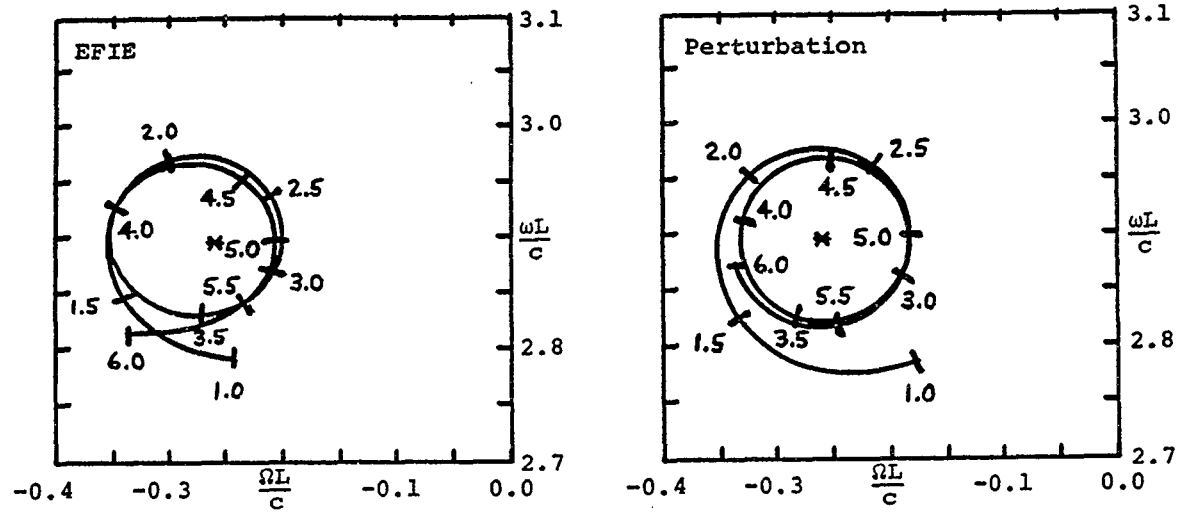

Figure 8.10 Trajectories of $\gamma_{as,1,1}L$ vs 2h/L for non-parallel, thin wire scatterers each oriented at an angle of 30° with respect to the plane of symmetry with L/a = 200. (2h/L varies from 1.0 to 6.0, "*" indicates location of natural frequency for isolated thin wire scatterer.)

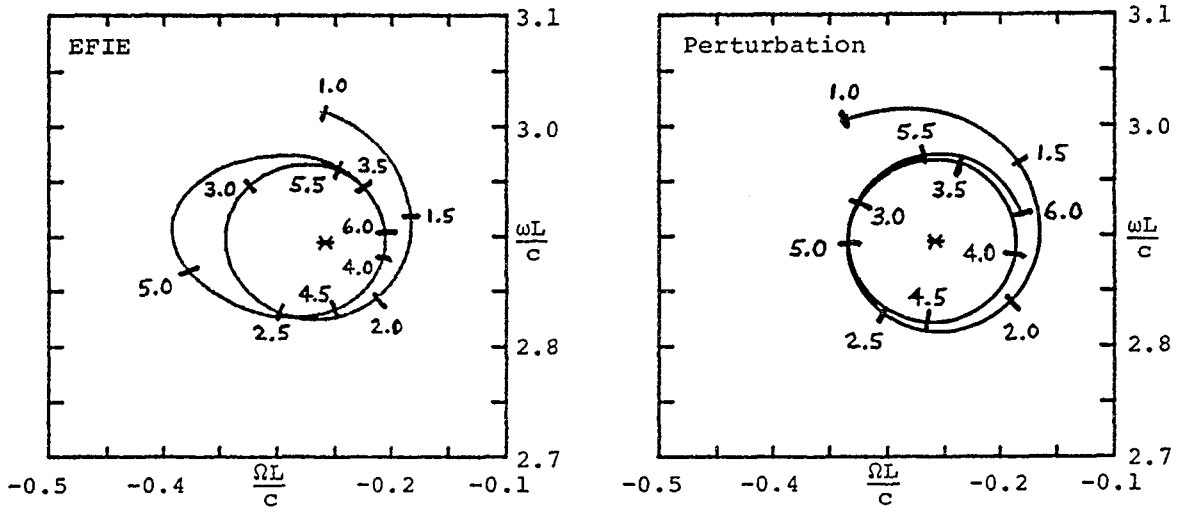

Figure 8.11 Trajectories of $\gamma_{sy,1,1}L$ vs 2h/L for non-parallel, thin wire scatterers each oriented at an angle of 30° with respect to the plane of symmetry with L/a = 200. (2h/L varies from 1.0 to 6.0, "*" indicates location of natural frequency for isolated thin wire scatterer.)

Table 8.1 Normalized image coefficient ($\frac{\mu_0 \nu_{1,1}}{4\pi L}$) associated with the dominant mode pole ($\gamma_{1,1}L = \frac{s_{1,1}L}{c}$) as a function of L/a and number of zones for two parallel, straight, thin wire scatterers.

L/a	Number of Zones	$\gamma_{1,1}L$	$\frac{\mu_0 \nu_{1,1}}{4\pi L} \times 10^2$
200	10	-0.2576 + j2.9092	4.6228 + j1.2232
	20	-0.2588 + j2.8946	4.7030 + j1.2542
	30	-0.2584 + j2.8864	4.7250 + j1.2613
	40	-0.2580 + j2.8812	4.7359 + j1.2644
	50	-0.2577 + j2.8774	4.7428 + j1.2661
	60	-0.2574 + j2.8746	4.7476 + j1.2673
	70	-0.2572 + j2.8723	4.7513 + j1.2682
	80	-0.2570 + j2.8704	4.7542 + j1.2688
	90	-0.2569 + j2.8687	4.7565 + j1.2693
	100	-0.2567 + j2.8674	4.7586 + j1.2697
400	10	-0.2264 + j2.9491	4.0260 + j0.9148
	20	-0.2281 + j2.9398	4.0921 + j0.9377
	30	-0.2280 + j2.9342	4.1087 + j0.9426
	40	-0.2279 + j2.9306	4.1167 + j0.9447
	50	-0.2277 + j2.9280	4.1214 + j0.9459
	60	-0.2276 + j2.9261	4.1245 + j0.9466
	70	-0.2274 + j2.9245	4.1269 + j0.9472
	80	-0.2273 + j2.9232	4.1285 + j0.9475
	90	-0.2272 + j2.9222	4.1303 + j0.9479
	100	-0.2272 + j2.9213	4.1314 + j0.9480
800	10	-0.2015 + j2.9774	3.5576 + j0.7073
	20	-0.2033 + j2.9716	3.6139 + j0.7247
	30	-0.2034 + j2.9675	3.6273 + j0.7283
	40	-0.2033 + j2.9649	3.6334 + j0.7299
	50	-0.2033 + j2.9631	3.6369 + j0.7307
	60	-0.2032 + j2.9617	3.6388 + j0.7311
	70	-0.2031 + j2.9606	3.6408 + j0.7315
	80	-0.2031 + j2.9597	3.6418 + j0.7317
	90	-0.2030 + j2.9590	3.6429 + j0.7319
	100	-0.2030 + j2.9584	3.6437 + j0.7321

Table 8.2 Normalized image coefficient ($\frac{\mu_0 \nu_{1,1}}{4\pi L}$) associated with the dominant mode pole ($\gamma_{1,1}L = \frac{s_{1,1}L}{c}$) as a function of orientation angle (ϕ) with L/a = 200 and 20 subsectional zones. ($\gamma_{1,1}L = -0.2588 + j2.8946$)

d	$\frac{\mu_0 \nu_{1,1}}{4\pi L} \times 10^2$
0	4.7030 + j1.2542
10	4.5475 + j1.2102
20	4.1049 + j1.0856
30	3.4407 + j0.9011
40	2.6486 + j0.6854
50	1.8327 + j0.4681
60	1.0909 + j0.2752
70	0.5037 + j0.1258
80	0.1287 + j0.0319
90	0 + j 0

Table 8.3 Normalized image coefficients for higher order poles vs ϕ.

ϕ	$\gamma_{1,2}L$	$\frac{\mu_0 \nu_{1,2}}{4\pi L} \times 10^2$
0	-0.3764 + j5.9591	0
10	"	-0.0845 - j0.0328
20	"	-0.2910 - j0.1120
30	"	-0.5084 - j0.1930
40	"	-0.6272 - j0.2339
50	"	-0.5964 - j0.2182
60	"	-0.4397 - j0.1580
70	"	-0.2330 - j0.0824
80	"	-0.0643 - j0.0225
90	"	0

ϕ	$\gamma_{1,3}L$	$\frac{\mu_0 \nu_{1,3}}{4\pi L} \times 10^2$
0	-0.4513 + j9.0089	0.5898 + j0.2462
10	"	0.4949 + j0.2038
20	"	0.2809 + j0.1099
30	"	0.0893 + j0.0302
40	"	0.0052 + j0.0002
50	"	0.0090 + j0.0067
60	"	0.0323 + j0.0177
70	"	0.0315 + j0.0158
80	"	0.0115 + j0.0055
90	"	0

ϕ	$\gamma_{1,4}L$	$\frac{\mu_0 \nu_{1,4}}{4\pi L} \times 10^2$
0	-0.4994 + j12.0100	0
10	"	-0.0826 - j0.0407
20	"	-0.2314 - j0.1117
30	"	-0.2845 - j0.1323
40	"	-0.2120 - j0.0930
50	"	-0.1028 - j0.0411
60	"	-0.0318 - j0.0108
70	"	-0.0057 - j0.0013
80	"	-0.0005 - j0.0000
90	"	0

☆ U.S. GOVERNMENT PRINTING OFFICE: 1987—773-134/61,030